REPORT DOCUMENTATION PAGE

PLEASE DO NOT RETURN YOUR FORM TO THE ABOVE ADDRESS.

1. REPORT DATE	2. REPORT TYPE	3. DATES COVERED
05/11/2010	Final Technical	12/01/07-11/30/09

4. TITLE AND SUBTITLE

Structural and Functional Mechanisms of Adaptations of WrbA in Extremophilic Organisms

5a. CONTRACT NUMBER

5b. GRANT NUMBER

FA9550-08-1-0013

5c. PROGRAM ELEMENT NUMBER

6. AUTHOR(S)

James G. Ferry

5d. PROJECT NUMBER

5e. TASK NUMBER

5f. WORK UNIT NUMBER

7. PERFORMING ORGANIZATION NAME(S) AND ADDRESS(ES)

Pennsylvania State University

8. PERFORMING ORGANIZATION REPORT NUMBER

9. SPONSORING/MONITORING AGENCY NAME(S) AND ADDRESS(ES)

AFOSR/RSL
875 N. Randolph St.,
Suite 325
Arlington, VA 22203-1768

10. SPONSOR/MONITOR'S ACRONYM(S)

11. SPONSOR/MONITOR'S REPORT NUMBER(S)

AFRL-OSR-VA-TR-2012-0019

12. DISTRIBUTION/AVAILABILITY STATEMENT

A (approved for public release; distribution is unlimited)

13. SUPPLEMENTARY NOTES

14. ABSTRACT

Properties of FMN-containing NADH:quinone oxidoreductases (WrbA) from the hyperthermophile Archaeoglobus fulgidus and the mesophile Escherichia coli were investigated to gain an understanding of the mechanisms by which proteins in extremophilic organisms adapt to high temperature. A model of the thermophilic enzyme was constructed based on the crystal structure of the mesophilic counterpart to guide experiments. An electrochemical cell was designed and constructed to probe the redox properties of FMN. Only subtle differences in the midpoint potential were recorded for the two enzymes consistent with congruent physiological functions. Contrary to redox potentials, the two proteins showed differences in FMN binding. Strong cooperativity in flavin binding for the mesophilic enzyme was dependent on the concentration of FMN whereas binding for the thermophilic enzyme was independent of ligand concentration. Comparison of enzyme activities between the two proteins with a variety of quinones suggested differences in the active site architecture accommodating electron acceptors. Properties of the mesophilic wild-type versus single amino acid substitution variants identified residues adjacent to FMN influencing the redox potential, oligomerization and enzyme

15. SUBJECT TERMS

thermophilic, flavoprotein, Archaeoglobus fulgidus, biosensor, biofuel cell

16. SECURITY CLASSIFICATION OF:			17. LIMITATION OF ABSTRACT	18. NUMBER OF PAGES	19a. NAME OF RESPONSIBLE PERSON
a. REPORT	b. ABSTRACT	c. THIS PAGE			James G. Ferry
					19b. TELEPHONE NUMBER: 814 404 7340

Form 298

20120918106

ABSTRACT

Properties of FMN-containing NADH:quinone oxidoreductases (WrbA) from the hyperthermophile *Archaeoglobus fulgidus* and the mesophile *Escherichia coli* were investigated to gain an understanding of the mechanisms by which proteins in extremophilic organisms adapt to high temperature. A model of the thermophilic enzyme was constructed based on the crystal structure of the mesophilic counterpart to guide experiments. An electrochemical cell was designed and constructed to probe the redox properties of FMN. Only subtle differences in the midpoint potential were recorded for the two enzymes consistent with congruent physiological functions. Contrary to redox potentials, the two proteins showed differences in FMN binding. Strong cooperativity in flavin binding for the mesophilic enzyme was dependent on the concentration of FMN whereas binding for the thermophilic enzyme was independent of ligand concentration. Comparison of enzyme activities between the two proteins with a variety of quinones suggested differences in the active site architecture accommodating electron acceptors. Properties of the mesophilic wild-type *versus* single amino acid substitution variants identified residues adjacent to FMN influencing the redox potential, oligomerization and enzyme activity. Both enzymes were suitable catalysts for biofuel cells and NADH-dependent amperometric NADH biosensors, although the thermophilic enzyme was found to be superior.

OBJECTIVES

Overall. The overarching goal of this proposal was to gain an understanding of the mechanisms by which proteins in extremophilic organisms adapt to extreme conditions, specifically high temperature. To this end, we proposed comparative studies of thermophilic and mesophilic homologues from the recently discovered flavin-containing NAD(P)H-dependent quinone reductase WrbA protein family. In addition to its role in survival and adaptation to stress, WrbA was chosen as a representative of the larger flavoprotein super family that constitutes a major portion of proteins in all prokaryotes. The overarching goal was an understanding of how the flavin environment of WrbA from the hyperthermophile *Archaeoglobus fulgidus* (AfWrbA) had evolved to stabilize and modulate properties of the flavin to function at high temperatures. The mesophilic WrbA chosen was from the model organism *Escherichia coli* (EcWrbA).

Year one (12/01/07-11/30/08). Goals for this year were to determine the crystal structure of AfWrbA and accumulate single amino acid replacement variants of both EcWrbA and AfWrbA providing a foundation on which to determine and compare factors that govern flavin redox chemistry, stability and oligomerization of both flavoproteins. Another goal was to develop instrumentation to determine the redox potentials of the wild-type and variant proteins.

Year two (12/01/08-11/30/09). Goals for this year were to characterize the wild-type and variant proteins with respect to redox properties of the flavin. Owing to lack of a crystal structure for AfWrbA and recognition of potential for the utility of WrbA proteins for developing a biosensor and fuel cell, a change in direction was implemented to pursue this line of investigation.

FINDINGS

Stability comparisons. To begin these studies, we established conditions for the reversible unfolding of EcWrbA and AfWrbA. Urea-induced unfolding in the absence of flavin revealed that AfWrbA is more stable than EcWrbA and the former refolds slower than the latter (Fig. 1). These results suggest that stabilization of AfWrbA occurs *via* both thermodynamic (increase in ΔG) and kinetic (slow unfolding rate) mechanisms. We planned to continue by investigating contributions to thermostability with various spectroscopic and biophysical methods in collaboration with Dr. George Makhatadze. One approach was *via* analysis of variant proteins in which amino acids were replaced by site directed mutagenesis. To this end, a fair amount of effort was expended overproducing both proteins in *E. coli*. Further, repeated attempts to crystallize AfWrbA were unsuccessful; thus, the structure of AfWrbA was modeled with the crystal structure of EcWrbA to guide this experimental approach (Fig. 2). Our plans for this aspect involved preparation of three variants: deleting residues D150-V154 and G167-R172 in EcWrbA, inserting sequences DVSQV and GGDGSR in AfWrbA, between residues 153/154 and 165/166 respectively and creating a quadruple variant S99E/G100R/A101R/E176Q in EcWrbA. Unfortunately, the collaboration with Dr. Makhatadze did not develop further which required a redirection of research as described in the following sections.

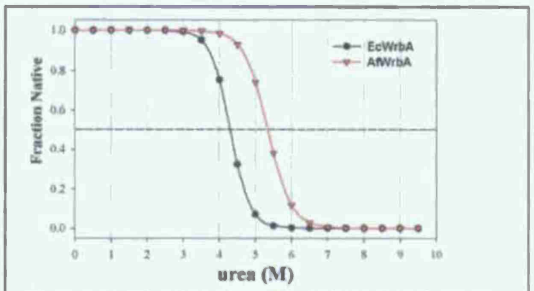

Figure 1. The fraction of native protein as a function of urea concentration monitored by changes in elipticity at 222 nm and 25°C.

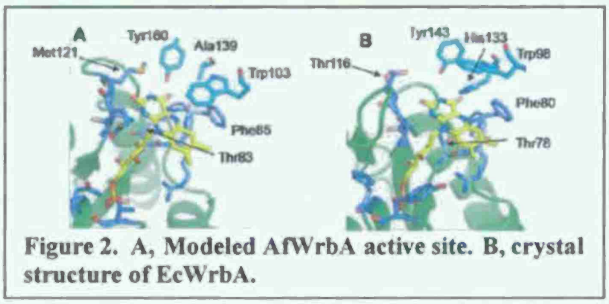

Figure 2. A, Modeled AfWrbA active site. B, crystal structure of EcWrbA.

Factors controlling flavin binding and oligomerization. EcWrbA and AfWrbA are tetrameric proteins that bind one flavin mononucleotide (FMN) per monomer. In general, the active sites adjacent to FMN were comparable with the notable exception of His133 present in EcWrbA that is absent in AfWrbA (Fig. 2). However, our initial focus was on the Phe80 residue in EcWrbA and the cognate Phe82 in AfWrbA suspected of having the greatest influence. Thus, the following variants of EcWrbA were obtained: Phe80Val, Phe80Ala, Phe80Gly, Phe80GlyGly, and Phe80Tyr. Visible spectra indicate that the variants have hypo- or hyper-chromic shifts in the first and second energy

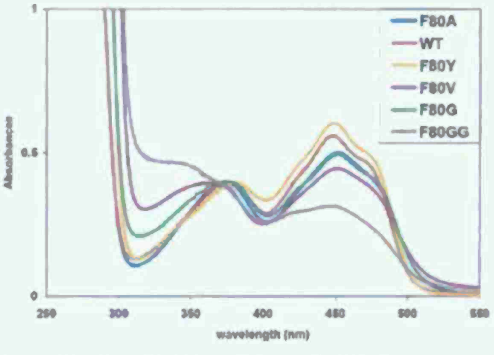

Figure 3. UV-visible spectra of wild-type EcWrbA and Phe80 variants.

transitions, and batho- or hypso-chromic shifts in the second energy transitions (Fig 3). In addition, each variant had different vibrational fine structure, which suggests that interactions with FMN are variant-dependent. In addition, analyses of these variants suggests Phe80 is important for oligomerization as dynamic light scattering showed Phe80GlyGly and Phe80Val do not participate in tetramerization whereas Phe80Gly retains the ability to form tetramers. These data suggest Phe80 is important for flavin binding and oligomerization.

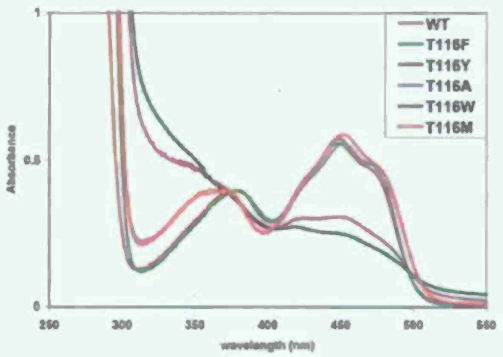

Figure 4. UV-visible spectra of wild-type EcWrbA and T116 variants.

Comparison of structures identifies Met118 of AfWrbA in the equivalent position of Thr116 in EcWrbA. To determine if this position is important in FMN binding and oligomerization, we cloned, over expressed, purified and analyzed five variants wherein Thr116 was replaced: Thr116Ala, Thr116Met, Thr116Trp, Thr116Phe, and Thr116Tyr. The UV-visible spectra indicate that several of the Thr116 variants displayed hypo- or hyper-chromic shifts in the first and second energy transitions, and batho- or hypso-chromic shifts in the second energy transitions (Fig 4). In addition, these variants also showed different vibrational fine structure. Variants with a significantly altered spectrum also showed decreased affinity for FMN suggesting a binding role for Thr116. Dynamic light scattering showed the Thr116Met and Thr116Trp variants retain the ability to form tetramers suggesting that Thr116 does not play a significant role in oligomerization.

The UV-visible spectra of oxidized and electrochemically-reduced wild-type EcWrbA and AfWrbA are shown in Figure 5. Although a spectral shift between the two proteins suggested possible variation in molecular orbital configuration, the results are consistent with flavoproteins that do not accumulate the one-electron reduced flavin semiquinone. The redox potentials of FMN in EcWrbA and AfWrbA were determined to further compare cofactor binding sites. This

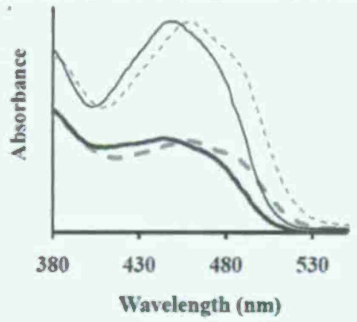

Figure 5. UV-visible spectra of oxidized and reduced EcWrbA and AfWrbA.

	$E_{m,6.5}$	ΔG	$\Delta\Delta G_{FMN}$	n
F80A	-181 ± 2	17.5	-1.4	1.19 ± 0.13
EcWrbA	-172 ± 5	16.6	-2.2	1.01 ± 0.13
T116A	-159 ± 2	15.3	-3.5	0.96 ± 0.07
Y143A	-156 ± 4	15.1	-3.8	0.97 ± 0.18
T78A	-155 ± 4	14.9	-3.9	0.96 ± 0.07
W98A	-152 ± 2	14.7	-4.1	0.84 ± 0.02
H133A	-148 ± 3	14.3	-4.5	2.30 ± 0.26

Table 1. Reduction potentials for wild-type EcWrbA and several alanine variants.

approach required construction of a specialized electrochemical cell with a small volume that limits diffusion distances from the electrode while retaining optical sensitivity *via* incorporating a longer (and variable) optical path length. The cell afforded reasonable speed and accuracy in

data collection, and the water-tight construction provided stability of the system longer than 24 hours. Voltage across the electrochemical cell was controlled with an EG&G PAR 273 potentiostat for data collection. The cell is essentially a clamp that ensures a water-tight seal to a gold-capillary electrode. An exploded view of the cell illustrates the basic construction (Figure 6). Detailed schematics are available to the scientific community sufficient for reproduction.

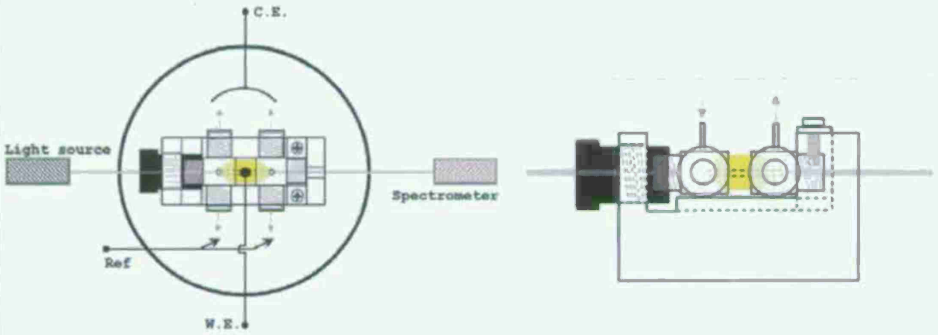

Figure 6. Views of the spectroelectrochemical cell. Left, top view of connections with the potentiostat, light source, and spectrometer. Abbreviations: counter electrode (C.E.), working electrode (W.E.) and reference electrode (Ref). Right, side view showing sample injection ports indicated by arrows.

Potentiometric titrations of wild-type EcWrbA (-172 mV ± 5.0) and AfWrbA (-158 mV ± 5.4) yielded similar redox potentials consistent with similar FMN-protein environments influencing the redox potential. The protein environment influencing the redox potential of FMN in EcWrbA was further investigated by replacing adjacent amino acids with alanine (Table1). Redox potentials for the T116A, H133A and T78A variants of EcWrbA were significantly less negative compared to the wild-type suggesting a role for these residues in modulating the redox potential. Nernst plots of the H133A variant data indicated a two-electron reduction, while all EcWrbA variants and the wild-type EcWrbA and AfWrbA proteins (not shown) appeared to participate in sequential one-electron reductions suggesting a role for this residue in stabilizing the two-electron reduced hydroquinone form in both proteins.

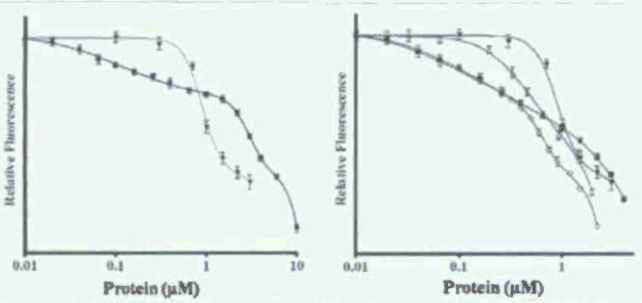

Figure 7. FMN binding assayed by fluorescence quenching. Left panel, saturating FMN. Symbols: (▼) EcWrbA, (■) AfWrbA. Right panel, limiting FMN. Symbols: (▼) wild type EcWrbA, (■) F80A variant, (Δ)W98A variant, (◇) T78A variant.

Contrary to redox properties, FMN binding assays indicated differences between EcWrbA and AfWrbA. Assays with saturating (150 μM) and limiting (5 μM) FMN are shown in Figure 7. Binding with apo-EcWrbA was dependent on flavin concentration and showed tighter affinity with saturated flavin. A single binding event was observed with either saturated or limited flavin, and the event was protein-dependent and appeared to correlate with

multimerization (not shown). Binding occurred with an apparent cooperativity of 4 with saturating FMN and an apparent cooperativity of 2 for limiting FMN. Cofactor binding with apo-AfWrbA had two transitions. Binding occurred with no cooperativity in the first transition and with an apparent cooperativity of 4 in the second transition. Both transitions were independent of flavin concentration under the tested conditions. Binding parameters for wild-type and variant proteins are shown in Table 2. Overall, fluorescence quenching with alanine variants indicated strong cooperativity in flavin binding for EcWrbA dependent on the ligand concentration for all except F80A which appeared to only bind flavin non-cooperatively and had the lowest cofactor affinity. Apparent cooperativity in flavin binding for AfWrbA was also strong, although no

	Saturated FMN		Limited FMN		Saturated FMN		Limited FMN	
	K_{S1}	K_{S2}	K_{L1}	K_{L2}	ΔG_{S1}	ΔG_{S2}	ΔG_{L1}	ΔG_{L2}
AfWrbA	^{1} 0.10 ± 0.03	^{4} 13.3 ± 0.6	^{1} 0.76 ± 0.08	^{4} 13.6 ± 0.1	-40.0	-27.8	-34.9	-27.8
EcWrbA		^{4} 0.82 ± 0.09		^{2} 16.8 ± 0.4		-34.7		-27.3
T116A		^{4} 0.66 ± 0.08		^{2} 14.8 ± 0.3		-35.3		-27.6
H133A		^{4} 0.62 ± 0.08		^{2} 18.6 ± 0.5		-35.4		-27.0
T78A	^{1} 0.11 ± 0.03	^{4} 0.43 ± 0.04		^{2} 22.3 ± 0.4	-39.7	-36.3		-26.6
Y143A		^{4} 0.25 ± 0.05		^{2} 26.1 ± 0.5		-37.7		-26.2
W98A		^{2} 0.44 ± 0.05		^{2} 28.0 ± 0.4		-36.3		-26.0
F80A	^{1} 0.13 ± 0.03			^{1} 39.4 ± 1.0	-39.3			-25.1

Table 2. Binding parameters for wild-type AfWrbA, wild-type EcWrbA and EcWrbA variants. Superscripts to the left of K values indicate cooperativity. K values are μM and G values are kJ/mol.

dependence on ligand concentration was observed. The EcWrbA T78A variant showed one transition with no cooperativity and a second transition with an apparent cooperativity of 4 similar to wild type AfWrbA.

To examine how residues adjacent to FMN contribute to enzyme activity, we assayed wild-type EcWrbA and alanine variants with various electron acceptors (Table 3). All of the alanine

	AfWT[a]	EcWT	H133A	T78A	T116A	Y143A	W98A	F80A
1,4-benzoquinone	4940 (270)[b]	660 (10)	650 (10)	390 (10)	150 (6)	270 (10)	180 (10)	50 (2)
1,4-naphthoquinone	3000 (30)	510 (10)	80 (2)	70 (1)	70 (3)	60 (2)	60 (1)	10 (0.1)
menadione	630 (20)	320 (10)	2.00 (0.04)	20 (0.01)	80 (3)	8.50 (0.2)	7.90 (0.1)	10 (1)
potassium ferricyanide	3970 (60)	180 (10)	180 (4)	150 (10)	140 (10)	140 (7)	110 (4)	59 (2)
2-hydroxy-1,4-naphthoquinone	2.90 (0.2)	3.80 (0.03)	N.D.	0.60 (0.01)	1.20 (0.02)	0.10 (0.01)	0.20 (0.02)	1.40 (0.1)
1,4-anthraquinone	380 (10)	7.90 (0.5)	0.80 (0.01)	0.70 (0.1)	0.50 (0.01)	0.70 (0.01)	0.80 (0.01)	1.00 (0.01)
8-hydroxyquinoline	0.30 (0.03)	0.10 (0.01)	0.10 (0.01)	0.10 (0.01)	0.10 (0.01)	0.10 (0.01)	0.20 (0.02)	0.20 (0.02)
9,10-anthraquinone	3.30 (0.4)	N.D.	0.20 (0.02)	precip.[d]	0.20 (0.01)	0.20 (0.05)	N.D.	0.20 (0.01)
9,10-anthraquinone-2-sulfonate	0.20 (0.01)	N.D.	N.D.	precip.	N.D.	0.80 (0.1)	N.D.	N.D.
9,10-anthraquinone-2,6-disulfonate	0.60 (0.03)	0.60 (0.01)	0.10 (0.01)	0.20 (0.01)	1.60 (0.03)	0.20 (0.01)	0.40 (0.02)	0.10 (0.02)
FMN	N.D.[c]	N.D.	N.D.	N.D.	N.D.	N.D.	N.D.	N.D.

[a] Average specific activities (micromoles · min^{-1} · mg^{-1})
[b] Standard Error
[c] N.D. = Not Detectable
[d] precip. = precipitation formed on reduction

Table 3. Specific activities of wild-type AfWrbA, wild-type EcWrbA and EcWrbA variants.

variants showed decreased activity with the electron acceptors compared to wild-type. Enzyme activities with smaller electron acceptors (1,4-benzoquinone and potassium ferricyanide) were slightly less affected among the variants. The general trend of the data indicates that F80A retained the least activity with the electron acceptors, further highlighting the importance of this

residue. The general retention of activity with 1,4-anthraquinone over 9,10-anthraquinones suggests that steric hindrance may influence substrate specificity. Therefore while WrbA proteins retain activity with a variety of electron acceptors, the activity appears to be limited by the substrate size and the functional group accessibility. Comparison of EcWrbA and AfWrbA wild-type showed a mixed trend in relative activities across electron acceptors consistent with differences in access to the active sites. Absolute activities are not comparable as both were assayed at 25°C, well below the growth temperature of 85°C for *A. fulgidus*.

AfWrbA and EcWrbA as new catalysts for NADH-dependent amperometric biosensors and biofuel cells. The enzymes were covalently linked to a low potential Os redox polymer onto graphite in the presence of single-walled carbon nanotube (SWCNT) preparations of varying average lengths. The performance of the enzyme for NADH oxidation was strongly

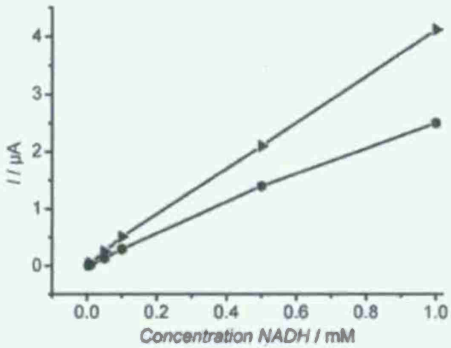

Figure 8. Comparison of the response of an AfWrbA and an EcWrbA/Os redox polymer modified electrode, blended with SWCNTs. Symbols: (▲) AfWrbA, (●) EcWrbA.

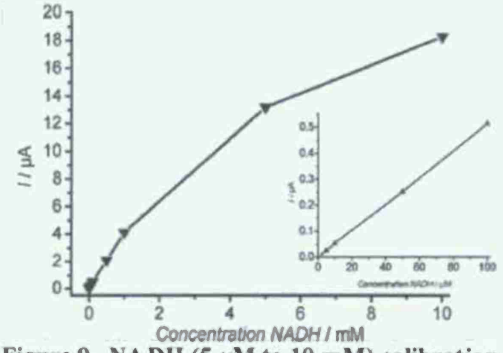

Figure 9. NADH (5 µM to 10 mM) calibration curves for an AfWrbA/Os redox polymer modified electrode blended with SWCNTs. Inset: 5 to 100 µM.

dependent on the average length of the applied SWCNTs. By blending the Os redox polymer with SWCNTs, the electrocatalytic current could be increased up to a factor of 5. Results obtained for AfWrbA modified electrodes were better than those for EcWrbA and provided excellent results (Figure 8). For an AfWrbA/Os redox polymer/SWCNTs modified electrode, the linear range for NADH detection was between concentrations of 5 μM and 1mM (Fig. 9). The limit of detection (LOD) was at 3 μM, and a sensitivity of 56.5 nA μM-1 cm-2 was calculated. Hence, the performance of the AfWrbA/Os redox polymer/SWCNT modified electrode was excellent and comparable to the diaphorase/Os redox polymer/SWCNT modified electrode (linear range, 5 μM-7 mM; LOD, 1 μM; sensitivity, 47.4 nA μM-1 cm-2).

Furthermore, the AfWrbA/Os redox polymer/SWCNTs modified electrode was used as an anode in combination with a Pt black cathode as a membraneless biofuel cell prototype with NADH as the fuel. The polarization curve and dependence of power density on the operating voltage are shown in Figure 10. The cell exhibited a maximum voltage (Vmax) of 300 mV, a maximum current density (J max) of 105 μA cm-2, and a maximum power density(Pmax) of 12 μW cm-2 at an operating voltage of 165 mV demonstrating the utility of AfWrbA to function in a membraneless biofuel cell opening future research efforts.

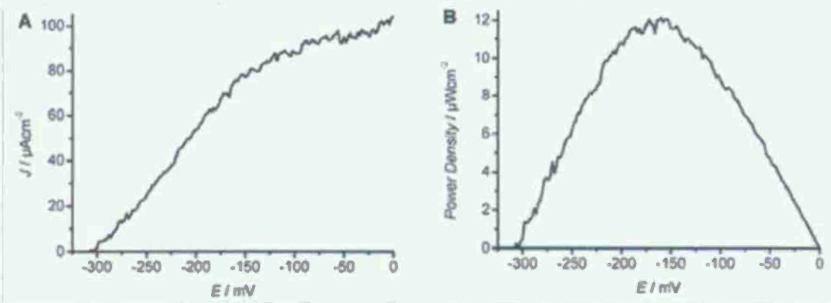

Figure 10. Panel A, polarization curve measured with linear sweep (0 to -350 mV) voltammetry. Panel B, dependence of the po wer density on the operating voltage.

COLLABORATIONS

Collaborators on the suitability of WrbA's as biosensors and biofuel cells were M. N. Zafar, F. Tasca and L. Gorton from Lund University, Sweden and G. Noll from the University of Siegen, Germany.

PUBLICATIONS

Zafar, M. N., F. Tasca, L. Gorton, E. V. Patridge, J. G. Ferry, and G. Noll. 2009. Tryptophan repressor-binding proteins from *Escherichia coli* and *Archaeoglobus fulgidus* as new catalysts for 1,4-dihydronicotinamide adenine dinucleotide-dependent amperometric biosensors and biofuel cells. Anal. Chem. **81**:4082-4088.

INTERACTIONS/TRANSITIONS

Our interaction with Dr. Uwe Slyter at the first AFOSR contractor meeting developed into a collaboration investigating the use of a carbonic anhydrase we discovered for immobilization onto S-layer proteins by Dr. Slyter as a means to capture carbon dioxide from point sources for mitigation of atmospheric levels.